Modeling Coupled 1D PDEs of Cardiovascular Flow with Spatial Neural ODEs

Hunor Csala
Department of Mechanical Engineering
Scientific Computing and Imaging Institute
University of Utah
Salt Lake City, UT 84112
hunor.csala@sci.utah.edu

Arvind Mohan
Computational Physics and Methods
Los Alamos National Laboratory
Los Alamos, NM 87545
arvindm@lanl.gov

Daniel Livescu
Computational Physics and Methods
Los Alamos National Laboratory
Los Alamos, NM 87545
livescu@lanl.gov

Amirhossein Arzani
Department of Mechanical Engineering
Scientific Computing and Imaging Institute
University of Utah
Salt Lake City, UT 84112
amir.arzani@sci.utah.edu

Abstract

Tackling coupled sets of partial differential equations (PDEs) through scientific machine learning presents a complex challenge, but it is essential for developing data-driven physics-based models. We employ a novel approach to model the coupled PDEs that govern the blood flow in stenosed arteries with deformable walls, while incorporating realistic inlet flow waveforms. We propose a low-dimensional model based on neural ordinary differential equations (ODEs) inspired by 1D blood flow equations. Our unique approach formulates the problem as ODEs in space rather than time, effectively overcoming issues related to time-dependent boundary conditions and PDE coupling. This innovative framework accurately captures flow rate and area variations, even when extrapolating to unseen waveforms. The promising results from this approach offer a different perspective on deploying neural ODEs to model coupled PDEs with unsteady boundary conditions, which are prevalent in many engineering applications.

1 Introduction

Coupled partial differential equations serve as a fundamental framework for describing a wide range of multi-physics phenomena in the natural world. Notably, cardiovascular flows exemplify the complex interplay of these equations, carrying significant real-world implications. Yet, accurately and efficiently modeling such phenomena poses considerable challenges. Here, we tackle the problem of blood flow in a stenosed artery with deformable walls, where the geometry is idealized but the problem is made reasonably complex by a realistic pulsatile inlet flow waveform and fluid-structure interaction (FSI). We create a low-dimensional model based on neural ordinary differential equations (NODEs) [2], inspired by the 1D blood flow equations. NODEs have been proven to be a versatile tool for scientific machine learning [9, 12] and fluid flow modeling [16, 15]. Data-driven approaches have shown promising results in the past [1] for cardiovascular applications, but NODEs have not yet been leveraged for blood flow problems. However, solving a coupled set of PDEs poses further challenges that have rarely been addressed in the literature. Namely, the solution of one PDE has to be fed into the other PDE, which demands solution smoothness and stability. We demonstrate that in

Machine Learning and the Physical Sciences Workshop, NeurIPS 2023.

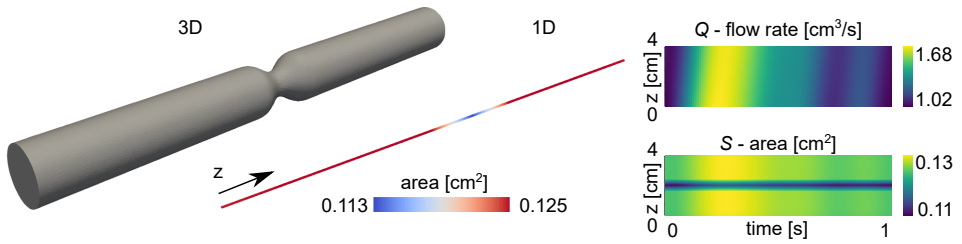

Figure 1: 3D and 1D models in stenosed arteries. Flow rate and area results from the 1D model for an example waveform are shown.

1D transport problems with periodic boundary conditions in time (pulsatile flow), an unprecedented reformulation of NODEs in space instead of the traditional temporal formulation, shows significant improvement in the stability of the trained coupled PDEs and their extrapolation accuracy.

2 Methods

2.1 Coupled PDEs for 1D Blood Flow Modeling

The one-dimensional equations for Newtonian, incompressible blood flow in a deforming, elastic vessel were derived in [5, 6]. They describe the flow with cross-sectionally averaged variables, defined along the centerline of the 3D geometry, where the unknowns are the flow rate Q, pressure p, and the cross-section area S:

$$\frac{\partial S}{\partial t} = -\frac{\partial Q}{\partial z} \tag{1}$$

$$\frac{\partial Q}{\partial t} = -(1+\delta)\frac{\partial}{\partial z}\left(\frac{Q^2}{S}\right) - \frac{S}{\rho}\frac{\partial p}{\partial z} + N\frac{Q}{S} + \nu\frac{\partial^2 Q}{\partial z^2}. \tag{2}$$

Equation 1 is the continuity equation, where t is time and z is the axial coordinate. Equation 2 is the single axial momentum balance equation, where ρ and ν are the blood density and kinematic viscosity respectively, both assumed to be constant. A time-varying parabolic velocity profile is assumed at the inlet, therefore the profile function parameters δ and N are given by the following relations [6]: $\delta = 1/3, N = -8\pi\nu$. A constitutive relationship is needed to close the above set of equations. Assuming an elastic wall model, a relationship between the cross-sectionally averaged pressure and the area was introduced in [11], considering the wall thickness and elastic modulus. A canonical stenosis geometry is chosen for this problem, and a time-dependent inlet flow rate waveform adds to the problem's complexity by being realistic. The outlet boundary condition is a resistance Windkessel element, often used in this application, with a reference pressure of $p_{ref} = 100$ mmHg. The 3D and derived 1D data can be seen in Fig. 1, with an example result for flow rate and area.

2.2 Machine Learning Approach

A popular approach for using NODEs to solve PDEs is to parameterize some, or even all, parts of the right-hand side of Eq. 2 with a neural network (NN). The PDEs would be spatially discretized with numerical methods and solved iteratively [4, 10]. This approach poses two significant challenges in the context of blood flow modeling (or, more broadly, non-stationary transport problems). First, the NODE has to incorporate the time-dependent boundary conditions. The prescribed time-dependent inlet flow rate boundary condition is the main driver of the physics in this problem, so it is crucial to introduce it accurately (not trivial for ODEs in time). Second, to solve the continuity equation, we need smooth, accurate predictions of both the flow rate Q and its spatial derivative $\partial Q/\partial z$. In the literature, most applications of NODEs include periodic boundary conditions in space [4, 10, 14], as implementing time-dependent boundary conditions is non-trivial and needs a customized differentiable ODE solver. An alternative is to parameterize the NODE such that the boundary condition appears as an extra input to the NN [8]. However, this lacks rigorous enforcement and is still practically challenging for time-dependent boundary conditions. We circumvented this issue by

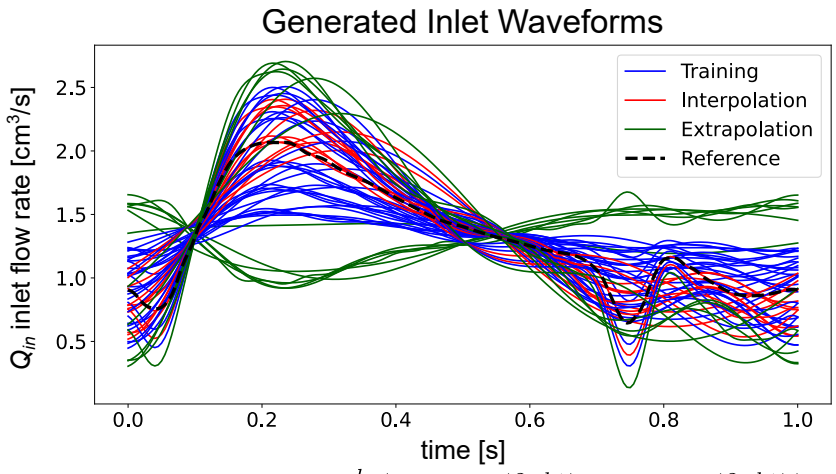

$$Q_{in}(t) = A_0 + \sum_1^k \left(aA_k \cos\left(\frac{2\pi kt}{T}\right) + B_k \sin\left(\frac{2\pi kt}{T}\right)\right)$$

$$k \in \{6, 9, 12, 15, 18, 59\} \quad a \in \{-2, 0.5, 0, 0.5, 1, 1.5, 1.75, 2, 2.5\}$$

Figure 2: Waveforms generated, colored by training, interpolation and extrapolation sets, along with the Fourier series equation and coefficient used for the different data sets.

developing a differentiable RK4 solver with the inlet boundary condition enforced after each timestep. While this achieved good predictions for Q (not shown here), it proved challenging to get *smooth* predictions of $\partial Q/\partial z$. This made the coupling of the NODE momentum equation with the continuity equation unstable, as incorrect $\partial Q/\partial z$ will always result in incorrect S. We present an approach to overcome both of the above issues simultaneously, by flipping the PDE in space and time, by solving it in space and discretizing time. The resulting spatial NODE model in space can be written as:

$$\frac{\partial Q}{\partial z} = NN_\theta(Q) \quad \text{and} \quad \frac{\partial S}{\partial t} = -\frac{\partial Q}{\partial z}. \tag{3}$$

Time is discretized into n_t timesteps, and an ODE is solved for each time instant in the spatial domain. Therefore, the above $Q \in \mathbb{R}^{n_t}$ represents a vector of flow rates, where each component is a time instant. Switching space and time enables accurate implementation of NODEs in this class of transport problems. Unlike many other NODE applications, such as Burgers' equation [10], Kuramoto-Sivashinksy [4, 10], Fisher-KPP equation [14], and homogeneous isotropic turbulence [16] where dynamics are periodic in space, cardiovascular flows are *periodic in time*, due to the pulsatile nature of the heartbeat. Esmaily and Jia [3] used a similar idea by computing Fourier transform in time, rather than space, for deriving efficient spectral formulations of blood flow problems. In our spatial formulation, the original inlet boundary condition becomes the initial condition for Q. The second advantage of space-time switching is that the solution Q is more likely to be implicitly smooth in the spatial direction z. This bypasses the above-mentioned issues by directly learning the $\partial Q/\partial z$ for coupling with the continuity equation.

The input vector size to the NN in Eq. 3 is the same as the temporal grid size, i.e. 101. The NN has 5 fully connected layers, with sizes of 101,10,10,10 & 101 respectively, and tanh activation functions, similar to related works [10, 4, 16]. To solve the NODE, we used the Tsit5 solver [17] from the Julia *DifferentialEquations.jl* library [13]. The NODE was trained using ADAM and BFGS optimizers, for a total of 10,000 epochs. The mean squared error loss function was used to compare the ground-truth flow rate Q and the NODE solution. The ODE solver used adaptive spatial step sizes, the loss was calculated at predefined n_z spatial gridpoints (for all n_t time instances), where the ground truth solution was available. Ground-truth values for S were not used in the training.

2.3 Data and Problem Setup

To test our approach, 54 different inlet flow rate waveforms were generated, using reference waveform from [7]. The variations were generated by fitting a Fourier-series and adjusting the number of components $k \in \{6, 9, 12, 15, 18, 59\}$ retained, and multiplying the cosine term by a coefficient a.

Table 1: Neural ODE results relative error.

Relative errors: $\|Y_{GT} - Y\|/\|Y_{GT}\|$			
Variable	Training	Interpolation	Extrapolation
Flow rate Q	0.44%	0.48%	0.66%
Area S	0.19%	0.22%	0.34%

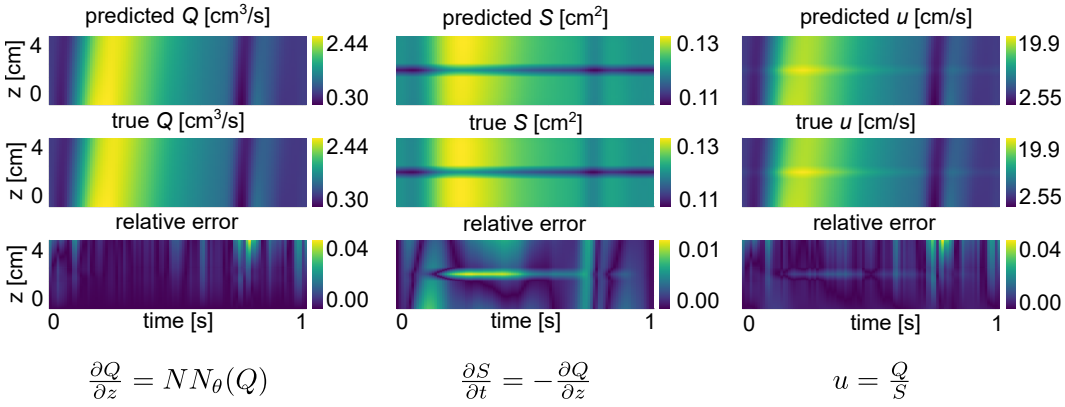

$$\frac{\partial Q}{\partial z} = NN_\theta(Q) \qquad \frac{\partial S}{\partial t} = -\frac{\partial Q}{\partial z} \qquad u = \frac{Q}{S}$$

Figure 3: Flow rate, area, velocity results, and relative errors visualized for a waveform from the extrapolation test set.

The period T was kept constant. Waveforms with $a \in \{-0.5, 0, 0.5, 1.5, 2\}$ were used for training, $a \in \{1, 1.75\}$ for testing interpolation capabilities, and $a \in \{-2, 2.5\}$ for testing extrapolation. These are shown in Fig. 2 with blue, red, and green colors respectively, along with the reference waveform with a dashed-black line. Some waveforms in the extrapolation set are qualitatively different than training and interpolation sets, therefore creating a realistic scenario for arbitrary new waveforms. 1D blood flow simulations were generated using SimVascular [18], an open-source finite-element method (FEM) solver, by solving equations 1 and 2. The stenosis geometry, material parameters, and all other settings were unchanged, and only the inlet boundary condition waveform was varied. The solution was saved every 0.01 seconds, leading to $n_t = 101$ timesteps, and $n_z = 100$ spatial locations for each simulation. All 1D simulations and NODE models were computed on a single Intel E5-2660 CPU.

3 Results

We are solving the coupled PDEs in Eq. 3, by using the NODE framework in space to obtain flow rate Q, which becomes an input to a classical ODE solver in time with finite-difference discretization in space to compute area S. Hence, the 1D axial velocity u can be directly obtained as $u = Q/S$. The model prediction from an extrapolation test is shown in Figure 3 for flow rate, area, and velocity, along with the corresponding point-wise relative errors. Since the ODEs were solved in space, the errors are higher further along the spatial direction. Nevertheless, the NODE model captures Q and its derivative well, and the predicted area S from the continuity equation is also accurate. The model also captures the increased velocities in the stenosed (blocked) region, and it is seen that the main driving factor for the temporal dynamics is the inlet boundary condition, which is effectively incorporated in our new formulation. The relative errors compared to the 1D FEM solutions from SimVascular are shown in Table 1. The relative error is defined as $\|Y_{GT} - Y\|/\|Y_{GT}\|$, where subscript GT stands for ground truth, $Y \in \{Q, S\}$ and $\|\cdot\|$ is the Frobenius norm. We notice excellent model performance, with all errors below 1%, while retaining its accuracy on both the interpolation and extrapolation cases.

4 Conclusions

Rapid patient-specific parametric blood flow modeling has the potential to revolutionize cardiovascular disease prevention and treatment. While the inherent uncertainties in boundary conditions make parametric studies a necessity, traditional PDE solvers often face challenges in providing accurate solutions within tight timeframes. To this end, we propose an approach to accurately model flow rate and area variations in coupled 1D blood flow equations with deformable walls and demonstrate extrapolation to unseen time-dependent inlet boundary condition waveforms. Casting the NODEs in space, rather than time, is shown to overcome two main challenges in non-stationary transport problems: First, it makes it easy to use different inlet boundary conditions as they are transformed to initial conditions in the neural ODE model. Second, it provides accurate derivatives in the spatial direction, enabling coupling with continuity equation, which directly depends on the $\partial Q/\partial z$ term. The presented approach is intended as a proof-of-concept, and a subsequent goal would be to train with 3D patient-specific FSI data and develop a fast and efficient NODE-based surrogate model capable of extrapolating to unseen waveforms, achieving better results than conventional 1D models. This would enable rapid parametric studies with a wide range of waveform shapes. Finally, we note that our NODE approach to learning a stable system of coupled PDEs with time-varying boundary conditions is generic and therefore expected to be applicable to a large class of unsteady transport problems far beyond cardiovascular flow.

5 Acknowledgements

The authors acknowledge funding from the LANL LDRD program office and the National Science Foundation (NSF) award #2247173. This work is approved for public release by the Los Alamos National Laboratory under LA-UR-23-31503.

References

[1] A. Arzani and S. T. Dawson. Data-driven cardiovascular flow modelling: examples and opportunities. *Journal of the Royal Society Interface*, 18(175):20200802, 2021.

[2] R. T. Chen, Y. Rubanova, J. Bettencourt, and D. K. Duvenaud. Neural ordinary differential equations. *Advances in neural information processing systems*, 31, 2018.

[3] M. Esmaily and D. Jia. A stabilized formulation for the solution of the incompressible unsteady stokes equations in the frequency domain. *Journal of Computational Physics*, 473:111736, 2023.

[4] M. Gelbrecht, N. Boers, and J. Kurths. Neural partial differential equations for chaotic systems. *New Journal of Physics*, 23(4):043005, 2021.

[5] T. J. Hughes. *A study of the one-dimensional theory of arterial pulse propagation*. Structural Engineering Laboratory, University of California, 1974.

[6] T. J. Hughes and J. Lubliner. On the one-dimensional theory of blood flow in the larger vessels. *Mathematical Biosciences*, 18(1-2):161–170, 1973.

[7] H. J. Kim, I. Vignon-Clementel, J. Coogan, C. Figueroa, K. Jansen, and C. Taylor. Patient-specific modeling of blood flow and pressure in human coronary arteries. *Annals of biomedical engineering*, 38:3195–3209, 2010.

[8] K. Lee and E. J. Parish. Parameterized neural ordinary differential equations: Applications to computational physics problems. *Proceedings of the Royal Society A*, 477(2253):20210162, 2021.

[9] R. Maulik, A. Mohan, B. Lusch, S. Madireddy, P. Balaprakash, and D. Livescu. Time-series learning of latent-space dynamics for reduced-order model closure. *Physica D: Nonlinear Phenomena*, 405:132368, 2020.

[10] H. Melchers, D. Crommelin, B. Koren, V. Menkovski, and B. Sanderse. Comparison of neural closure models for discretised pdes. *Computers Mathematics with Applications*, 143: 94–107, 2023. ISSN 0898-1221. doi: https://doi.org/10.1016/j.camwa.2023.04.030. URL https://www.sciencedirect.com/science/article/pii/S0898122123001736.

[11] M. S. Olufsen. Structured tree outflow condition for blood flow in larger systemic arteries. *American journal of physiology-Heart and circulatory physiology*, 276(1):H257–H268, 1999.

[12] G. D. Portwood, P. P. Mitra, M. D. Ribeiro, T. M. Nguyen, B. T. Nadiga, J. A. Saenz, M. Chertkov, A. Garg, A. Anandkumar, A. Dengel, et al. Turbulence forecasting via neural ode. *arXiv preprint arXiv:1911.05180*, 2019.

[13] C. Rackauckas and Q. Nie. Differentialequations.jl–a performant and feature-rich ecosystem for solving differential equations in julia. *Journal of Open Research Software*, 5(1):15, 2017.

[14] C. Rackauckas, Y. Ma, J. Martensen, C. Warner, K. Zubov, R. Supekar, D. Skinner, A. Ramadhan, and A. Edelman. Universal differential equations for scientific machine learning. *arXiv preprint arXiv:2001.04385*, 2020.

[15] C. J. G. Rojas, A. Dengel, and M. D. Ribeiro. Reduced-order model for fluid flows via neural ordinary differential equations, 2021.

[16] V. Shankar, G. D. Portwood, A. T. Mohan, P. P. Mitra, D. Krishnamurthy, C. Rackauckas, L. A. Wilson, D. P. Schmidt, and V. Viswanathan. Validation and parameterization of a novel physics-constrained neural dynamics model applied to turbulent fluid flow. *Physics of Fluids*, 34(11), 2022.

[17] C. Tsitouras. Runge–kutta pairs of order 5 (4) satisfying only the first column simplifying assumption. *Computers & Mathematics with Applications*, 62(2):770–775, 2011.

[18] A. Updegrove, N. M. Wilson, J. Merkow, H. Lan, A. L. Marsden, and S. C. Shadden. Simvascular: an open source pipeline for cardiovascular simulation. *Annals of biomedical engineering*, 45:525–541, 2017.